Diameter distribution of single wall carbon nanotubes in nanobundles

Stéphane Rols, Ariete Righi, Laurent Alvarez, Éric Anglaret, Robert Almairac, Catherine Journet, Patrick Bernier, Jean-Louis Sauvajol, Ana Benito, Wolfgang K. Maser, et al.

Eur. Phys. J. B **18**, 201–205 (2000)

THE EUROPEAN PHYSICAL JOURNAL B

EDP Sciences

Diameter distribution of single wall carbon nanotubes in nanobundles

S. Rols[1,2], A. Righi[1], L. Alvarez[1], E. Anglaret[1], R. Almairac[1], C. Journet[1], P. Bernier[1], J.L. Sauvajol[1,a], A.M. Benito[3], W.K. Maser[3], E. Muñoz[3], M.T. Martinez[3], G.F. de la Fuente[4], A. Girard[5], and J.C. Ameline[5]

[1] Groupe de Dynamique des Phases Condensées[b], Université Montpellier II, 34095 Montpellier Cedex 5, France
[2] Institut Laue-Langevin, 38042 Grenoble, France
[3] Instituto de Carboquimica, CSIC, Zaragoza 50015, Spain
[4] Instituto de Ciencia de Materiales de Aragón, Zaragoza 50015, Spain
[5] Groupe Matière Condensée et Matériaux, Campus de Beaulieu, 35042 Rennes, France

Received 22 December 1999 and Received in final form 17 July 2000

Abstract. The frequency of the Raman active A_{1g} radial breathing mode has been widely used as a tool to estimate the distribution of diameters of single wall carbon nanotubes (SWNT). However, the relation between frequency and diameter is not straightforward and results are model-dependent. Because most of the experiments are performed on bundles and not on isolated tubes, the model should especially take into account the van der Waals intertube interactions. Here, we use a pair-potential approach to account for such interactions and we derive a nonlinear relation between the SWNT diameter and the frequency of the A_{1g} radial breathing modes. We demonstrate a good agreement between calculations and the diameters derived from diffraction experiments *on the same samples*.

PACS. 78.30.Na Fullerenes and related materials – 63.22.+m Phonons in low-dimensional structures and small particles

1 Introduction

Raman scattering has been shown to be a powerful tool to probe the structure, diameter and electronic properties of single wall nanotubes (SWNT) [1–8]. It has been experimentally demonstrated that Raman scattering is dominated by a resonant process which has been associated with optical transitions between 1D states in the electronic band structure [2,6,7]. In the low-frequency range (100 to 300 cm^{-1}) the measurement of the A_{1g} radial breathing mode (RBM) is a convenient way of probing the SWNT diameter distribution [2–11]. However, no clear quantitative agreement has been found between the distribution of diameters estimated by Raman and other techniques, such as diffraction or electron microscopy [8,12]. The study of the distribution of tube diameters from the frequency of the RBM is actually not straightforward because (i) the relation between the tube diameter and the RBM frequency for an isolated tube is model-dependent, (ii) for tubes assembled into bundles, it is necessary to take into account the intertube interaction to derive properly this relation. Here, we calculate the relation between the RBM and the tube diameter using a force constant model for the intratube dynamics and an additional Lennard-Jones potential to account for van der Waals intertube interactions in infinite bundles. This allows a good agreement to be obtained between the diameter distribution derived from the profile of the Raman spectrum in the RBM range and that derived from the analysis of diffraction patterns *on the same samples*.

2 Experimental

Different nanotube samples were used in this study in order to cover a large range of tube diameters. Some samples were prepared *via* the solar route in an Ar atmosphere using Y_2O_3 as catalyst [11,13] (sample a), *via* a cw-CO_2 laser ablation technique in an Ar atmosphere using a Ni/Y catalyst mixture [14] (sample b), or *via* the electric arc discharge technique in a He atmosphere using a Ni/Y catalyst mixture [15] (sample c). Sample d was supplied by Tubes@Rice (Houston, Texas) [16].

Room-temperature neutron diffraction (ND) experiments were performed on the G6-1 diffractometer at the Laboratoire Léon Brillouin (Saclay, France) using incident neutrons of wavelength $\lambda = 4.73$ Å. X-ray diffraction (XRD) experiments were performed at GDPC using the K_α radiation ($\lambda = 1.542$ Å) of a Cu anticathode and on the diffractometer WDIF4C at LURE (Orsay, France). Raman spectra were measured using the 514.5 nm excitation

[a] e-mail: sauva@gdpc.univ-montp2.fr
[b] UMR CNRS 5581

line from an Ar ion laser (Spectra physics 2000) and the 647.1 nm excitation from a mixed Ar/Kr ion laser (Spectra physics 2017) in the back scattering geometry on a Jobin-Yvon T64000 spectrometer equiped with a liquid nitrogen cooled CCD detector.

3 Results

3.1 Diffraction measurements and calculations

The diffraction patterns are found to be significantly different for all samples (solid lines in Fig. 1, top). The calculations of such patterns have been reported elsewhere [12,17]. The organisation of the tubes into bundles is manifested by the presence of peaks below 2 $Å^{-1}$. The most intense peak is observed at the lowest Q and corresponds to the (10) Bragg reflexion from the hexagonal 2D lattice of tubes. For samples a and b, the (10) peak is located around 0.33–0.34 $Å^{-1}$. However, it is much broader for sample b. The (10) peak is shifted upward to 0.44–0.45 $Å^{-1}$ for samples c and d. However, the relative intensities of the other diffraction peaks are significantly sample-dependent. Calculations on the basis of the model presented in reference [17] were performed in order to fit the data (dashed lines in Fig. 1, top). The distribution of diameters was assumed to be a Gaussian, truncated for diameters smaller than 0.67 nm (the diameter of C_{60} which is also the smallest diameter expected for capped SWNT). Best agreements are obtained for mean-diameters of 1.92 nm (HWHM = 0.15 nm), 1.41 nm (0.5), 1.36 nm (0.15) and 1.24 nm (0.15) for samples a, b, c and d respectively.

3.2 Relation between RBM frequency and SWNT diameter

The frequency of the A_{1g} RBM is very sensitive to the tube diameter. The frequency of the RBM in an isolated tube was estimated by several groups using a force constant model [8,18,19], a tight binding approach [2,20,21] or an *ab initio* method [9]. As far as isolated tubes are concerned, the RMB frequency follows a linear dependence on the inverse of the diameter:

$$\nu\,(\mathrm{cm}^{-1}) = A/d\,(\mathrm{nm}). \qquad (1)$$

The value of the prefactor A is model-dependent: the RBM frequency for a (10,10) tube is calculated to be 157 cm^{-1} in reference [21], 165 cm^{-1} in the force constant model [8,18,19] (*i.e.* $A = 224\,\mathrm{nm\,cm}^{-1}$), 175 cm^{-1} in reference [9] and 195 cm^{-1} in reference [20]. This broad dispersion in the RBM frequencies illustrates that the estimation of SWNT diameters from the frequencies is not straightforward. On the other hand it is well established that in most SWNT samples, the nanotubes self-assemble into bundles [13–15]. Because of its radial character, the RBM is likely to be much influenced by the nanotube packing. Consequently, in order to derive a relation between the RBM frequencies and the tube diameter in bundles, it is necessary to take into account the intertube coupling. We calculated the RBM frequency of an infinite crystal of identical and infinitely long nanotubes by considering a Lennard-Jones potential $U(R) = 4\varepsilon[\sigma/R^{12} - \sigma/R^{6}]$ in addition to a force constant model in order to account for the van der Waals intertube interactions. We used the same van der Waals parameters, $\varepsilon = 2.964$ meV and $\sigma = 3.407$ Å, as Lu and Wang [22] which provide the best fits for the interlayer distance and the C_{33} elastic constant of graphite and well describe the bulk properties of solid C_{60} as well [23]. Details of the calculations are reported elsewhere [19]. The results reported in Figure 2 compare the RBM frequencies for isolated tubes and tubes in infinite bundles. A difference of about 16 cm^{-1} is found for a (10,10) tube, in good agreement with the 14 cm^{-1} calculated in another work for a (9,9) tube [24]. Note that the relation between the RBM frequency and the inverse of the SWNT diameter is no longer linear. The best fit (solid line in Fig. 2) is achieved with the following phenomenological scaling law [19]:

$$\nu\,(\mathrm{cm}^{-1}) = 238/d\,(\mathrm{nm})^{0.93}. \qquad (2)$$

We emphasize that in the "typical" range of SWNT diameters (1.2–2 nm), equation (1) provides a satisfactory fit of the data (dashed line in Fig. 2) with $A = 243\,\mathrm{nm\,cm}^{-1}$. However, the linear fit deviates from the data for small diameters.

3.3 Raman measurements

Raman experiments were performed on samples a to d, *the same samples as were studied in diffraction*. The results are presented in Figure 1 (bottom). They are significantly different for all samples. Raman scattering from SWNT is a resonant process associated with allowed optical transitions (AOT) between singularities in the electronic density of states. Therefore, different tubes are selectively excited at different excitation-laser energies as a function of their AOT, *i.e.* of their diameter and semi-conducting or metallic character [6,11]. Consequently, experiments with different laser energies must be carried out in order to estimate the distribution of SWNT diameters. This is illustrated by the differences between the Raman spectra excited at 2.41 eV (dashed lines) and 1.92 eV (solid lines). The frequency of the major peaks is reported in Table 1.

It is not straightforward to derive the distribution of tube diameters from the intensity of the RBM peaks because of resonance effects. On the other hand, one can estimate the mean RBM frequency from an arithmetic average of the frequencies of the main RBM peaks. We find 128 cm^{-1} for sample a, 174 cm^{-1} for sample b, 183 cm^{-1} for sample c and 192 cm^{-1} for sample d. Using equation (2), this leads to mean-diameters of about 1.95, 1.40, 1.33 and 1.26 nm, respectively, in good agreement with the diffraction results (Tab. 2). Note that the most significant differences between samples b and c are observed at 1.92 eV.

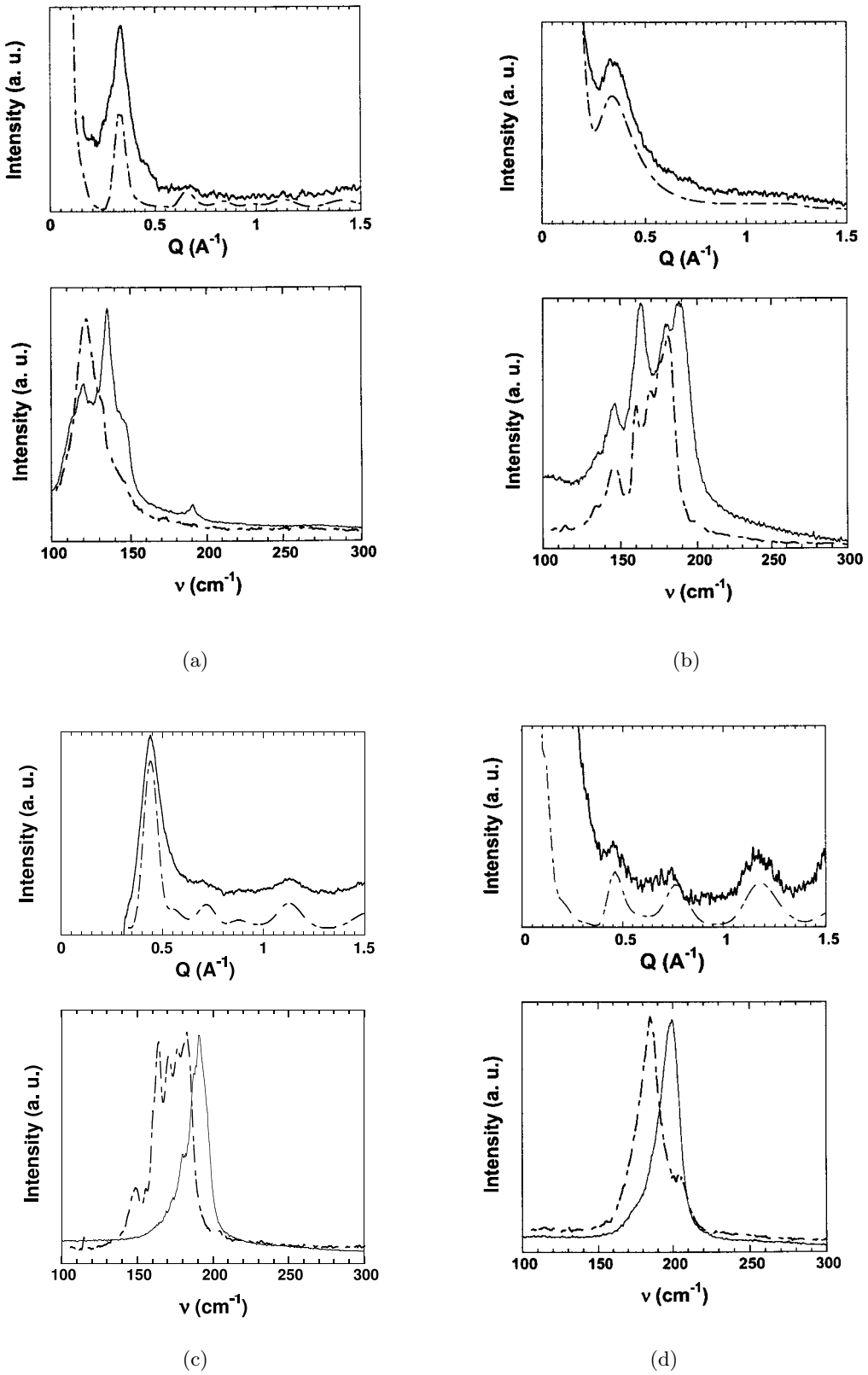

Fig. 1. Diffraction patterns (top) and Raman spectra (bottom) for samples a to d. The diffraction data are in solid lines and calculations in dashed lines. Raman spectra are measured with two different laser energies: 2.41 eV (dashed lines) and 1.92 eV (solid lines).

Table 1. Frequencies of the major A_{1g} RBM measured for each sample for laser energy 2.41 eV (*) and/or 1.92 eV ($^{\#}$).

Sample a	*121$^{\#}$	135$^{\#}$								
Sample b			*146$^{\#}$	*161	163$^{\#}$	*170		*180$^{\#}$	189$^{\#}$	
Sample c					*164	*171	*177	*182	191$^{\#}$	*198$^{\#}$
Sample d								*185		199$^{\#}$

Table 2. Corresponding SWNT diameters (nm) calculated from equation (2) compared to the dispersion of diameters derived from the analysis of the XRD patterns.

	Mean RBM frequency	Mean SWNT diameter from equation (1)	Mean SWNT diameter from equation (2)	Mean SWNT diameter from diffraction
Sample a	128 cm^{-1}	1.75 nm	1.95 nm	1.92 nm
Sample b	168 cm^{-1}	1.33 nm	1.45 nm	1.41 nm
Sample c	181 cm^{-1}	1.24 nm	1.34 nm	1.36 nm
Sample d	192 cm^{-1}	1.17 nm	1.26 nm	1.24 nm

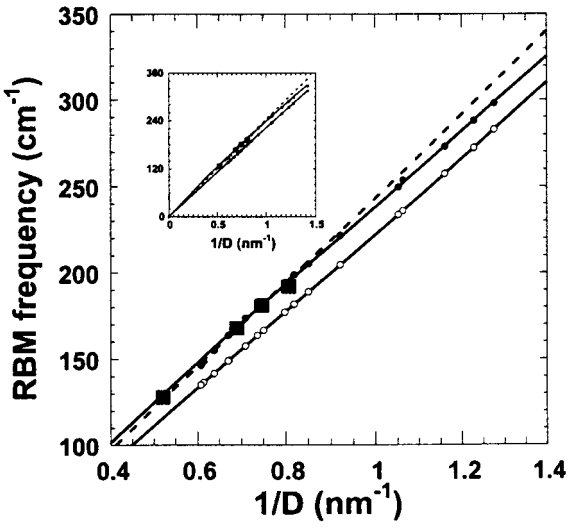

Fig. 2. SWNT diameter dependence of the A_{1g} RBM frequency for isolated tubes (○) and tubes assembled into infinite bundles (●). The solid lines are best fits to the data (Eqs. (1, 2)). The dashed straight line is a fit of the (●) data to equation (1). The symbols (■) correspond to the mean-Raman frequency of the RBM for samples a to d, whose mean-diameter was estimated from the diffraction patterns.

The observation of low-frequency peaks for the laser-ablation sample is ascribed to a much larger amount of tubes with large diameters, between 1.6 nm and 1.8 nm, in agreement with the much larger polydispersity detected in diffraction. In Figure 2 (full squares) we report the RBM frequency measured on samples a to d *versus* the inverse of the diameter derived from the diffraction patterns. A good agreement with the prediction of our model (relation (2)) is found.

In Table 2, we also reported the mean-diameter calculated from equation (1) in the force constant model. The results are systematically underestimated as compared to the diffraction data. The Raman results are found to be in much better general quantitative agreement with the diffraction data using equation (2), *i.e. by considering the van der Waals interactions between tubes* in the calculations. Consequently, relation (2) appears to be a useful tool to derive the SWNT diameter distribution from the RBM spectra. However, Raman and diffraction studies on bundles of tubes of sufficiently small diameters will be necessary to provide a definitive confirmation of the validity of our approach. Alternatively, comparison between Raman studies on bundles of tubes and isolated tubes of the same diameters would also provide a relevant test of the model. This will be a challenge for future synthesis of SWNT samples.

4 Conclusion

Diffraction and Raman measurements on bundles of SWNT with various diameters were performed *on the same samples*. The diameter dispersion of the nanotubes for each sample was derived from the analysis of the diffraction patterns. A good agreement is found with diameters calculated from the RBM frequencies using a nonlinear expression which accounts for van der Waals intertube interactions in the bundles.

We thank the Laboratoire Léon Brillouin (LLB) and the Laboratoire pour l'Utilisation du Rayonnement Électromagnétique (LURE) for providing neutron and X-ray beam time. We acknowledge I. Mirebeau (LLB) and J.P. Lauriat and E. Elkaim (LURE) for their assistance in the diffraction experiments. S.R. acknowledges the Région Languedoc-Roussillon for financial support. A.R. acknowledges financial support from the Brazilian agency CNPq.

References

1. A. Kasuya, M. Sugano, T. Maeda, Y. Saito, K. Tohji, H. Takahashi, Y. Sasaki, M. Fukushima, Y. Nishina, C. Horie, Phys. Rev. B **57**, 4999 (1997).
2. A.M. Rao, E. Richter, S. Bandow, B. Chase, P.C. Eklund, K.A. Williams, S. Fang, K.R. Subbaswamy, M. Menon, A. Thess, R.E. Smalley, G. Dresselhaus, M.S. Dresselhaus, Science **275**, 187 (1997).
3. M. Sugano, A. Kasuya, K. Tohji, Y. Saito, Y. Nishina, Chem. Phys. Lett. **292**, 575 (1998).
4. M. Lamy de la Chapelle, S. Lefrant, C. Journet, W.K. Maser, P. Bernier, A. Loiseau, Carbon **36**, 705 (1998).
5. M.A. Pimenta, A. Marucci, S.D.M. Brown, M.J. Matthews, A.M. Rao, P.C. Eklund, R.E. Smalley, G. Dresselhaus, M.S. Dresselhaus, J. Mater. Res. **13**, 2396 (1998); M.A. Pimenta, A. Marucci, S.A. Empedocles, M.G. Bawendi, E.B. Hanlon, A.M. Rao, P.C. Eklund, R.E. Smalley, G. Dresselhaus, M.S. Dresselhaus, Phys. Rev. B **58**, R16016 (1998).
6. H. Kataura, Y. Kumazawa, Y. Maniwa, I. Umezu, S. Suzuki, Y. Ohtsuka, Y. Achiba, Synth. Met. **103**, 2555 (1999).
7. E. Richter, K.R. Subbaswany, Phys. Rev. Lett. **79**, 2738 (1997).
8. S. Bandow, S. Asaka, Y. Saito, A.M. Rao, L. Grigorian, E. Richter, P.C. Eklund, Phys. Rev. Lett. **80**, 3779 (1998).
9. J. Kürty, G. Kresse, H. Kuzmany, Phys. Rev. B **58**, R8869 (1998).
10. E. Anglaret, N. Bendiab, T. Guillard, C. Journet, G. Flamant, D. Laplaze, P. Bernier, J.L. Sauvajol, Carbon **36**, 1815 (1998).
11. L. Alvarez, A. Righi, T. Guillard, S. Rols, E. Anglaret, D. Laplaze, J.L. Sauvajol, Chem. Phys. Lett. **316**, 186 (2000).
12. E. Anglaret, S. Rols, J.L Sauvajol, Phys. Rev. Lett. **81**, 4780 (1998).
13. L. Alvarez, T. Guillard, J.L. Sauvajol, G. Flamant, D. Laplaze, Appl. Phys. A **70**, 169 (2000).
14. W.K. Maser, E. Munoz, A.M. Benito, M.T. Martinez, G.F. de la Fuente, Y. Maniette, E. Anglaret, J.L. Sauvajol, Chem. Phys. Lett. **292**, 587 (1998).
15. C. Journet, W.K. Maser, P. Bernier, A. Loiseau, M. Lamy de la Chapelle, S. Lefrant, P. Deniard, R. Lee, J.E. Fischer, Nature **388**, 756 (1997).
16. A. Thess, R. Lee, P. Nicolaev, H. Dai, P. Petit, J. Robert, C. Xu, Y.H. Lee, S.G. Kim, D. Colbert, G. Scuseria, D. Tomanek, J.E. Fisher, R.E. Smalley, Science **273**, 487 (1996).
17. S. Rols, R. Almairac, L. Henrard, E. Anglaret, J.L. Sauvajol, Eur. Phys. J. B **10**, 263 (1999).
18. R. Saito, T. Takeya, T. Kimura, G. Dresselhaus, M.S. Dresselhaus, Phys. Rev. B **57**, 4145 (1998).
19. S. Rols (unpublished results).
20. L. Henrard, E. Hernandez, P. Bernier, A. Rubio, Phys. Rev. B **60**, R8521 (1999).
21. D. Kahn, J. Ping Lu, Phys. Rev. B **60**, 6535 (1999).
22. J.P. Lu, W. Yang, Phys. Rev. B **49**, 11421 (1994).
23. J.P. Lu, X-P. Li, R.M. Martin, Phys. Rev. Lett. **68**, 1551 (1992).
24. U.D. Vankateswaran, A.M. Rao, E. Richter, M. Menon, A. Rinzler, R.E. Smalley, P.C. Eklund, Phys. Rev. B **59**, 10928 (1999).